UNIVERSITÄT
BAYREUTH

Master Thesis

Stabilizing Global Simulation in GKW by the Introduction of the Parallel Electric Field $E_{\parallel}$

Manuel Lippert

Submission date: November 22, 2023

Physics Department at the University of Bayreuth

Supervisors:
Prof. Arthur G. Peeters
Dr. Florian Rath

★ 07.07.2020

This thesis is dedicated to my cat **Leo**
who is part of our family since July 2020.
He is the kindest cat I ever own and very playful.
For a long life together.

I love you.

Manuel Lippert
November 22, 2023

Acknowledgement

First, I would like to extend my greatest gratitude to my supervisor Prof. Arthur Peeters and Dr. Florian Rath. I would like to thank both of you for your guidance and support during the submission process of the brief communication and the helping hands during the writing process of this thesis and development of the restart script.

I would like to thank Bernhard Winkler and Markus Hilt for the great technical support regarding my questions to the `btrzx1`-cluster which helped me develop the restart script as it is now.

Also, I would like to thank my best friend, Paul Schwanitz, for his support in many situations and the good discussions in- and outside of academia. In addition I would like to thank Anna-Maria Pleyer, Dominik Müller and Stefan Barthelmann for the great time of sharing the office together.

I thank Anna-Maria Pleyer and my sister Cornelia Lippert for proofreading this thesis and brief communication, which helps me getting better at English spelling.

Outside of academia, I would like to extend my gratitude to my parents, my brother, his wife and daughter, my sister and my girlfriend for their encouragement, endurance and support while writing this thesis.

Abstract

Ion temperature gradient-driven turbulence (ITG) close to marginal stability exhibits zonal flow pattern formation on mesoscales, so-called $\mathrm{E} \times \mathrm{B}$ staircase structures. Such pattern formation has been observed in local gradient-driven flux-tube simulations as well as global gradient-driven and global flux-driven studies.

To reduce the computational effort for the simulations lower input parameter of GKW (Gyro Kinetic Workshop) were tested to find the optimum of minimum resolution for the performed simulations.

For convenience, a `python` script (`slurm_monitor.py`) was written to monitor the simulation on the `btrzx1`-cluster and start/restart until the completion criterion is fulfilled.

Furthermore, it is shown by multiple box size convergence scans that a mesoscale pattern size of $\sim 57 - 76\,\rho_{\mathrm{th}}$ is inherent to ITG-driven turbulence with Cyclone Base Case parameters in the local limit. This outcome also implies that a typical scale for avalanche-like transport is inherent to ITG-driven turbulence.

Zusammenfassung

Ionen-Temperaturgradienten getriebene Turbulenzen (ITG) weisen nahe niedriger Stabilität Zonal Flow Strukturbildungen, sogenannte $\mathrm{E} \times \mathrm{B}$ Treppenstrukturen, auf Mesoskalen auf. Solche Strukturbildungen wurden sowohl in lokal gradientengetriebene Flussschlauchsimulationen als auch in global gradientengetriebenen und global flussgetriebenen Untersuchungen entdeckt.

Um den Aufwand der Berechnungen der Simulationen zu reduzieren wurden mehrere kleinere Inputparameter für GKW (Gyro Kinetic Workshop) getestet um die optimal kleinste Auflösung für die ausgeführten Simulationen zu finden.

Der Einfachheit halber wurde ein `python`-Skript (`slurm_monitor.py`) geschrieben, was Simulationen auf den `btrzx1`-Cluster überwacht und gegebenenfalls startet/neustartet bis das Kriterium zur Vollendung erfüllt ist.

Weiterhin wurde doch mehrere radiale konvergierende Boxgrößen-Scans gezeigt, dass eine Mesoskalengröße von $\sim 57 - 76\,\rho_{\mathrm{th}}$ inhärent zur ITG getriebenen Turbulenz mit Cyclone Base Parameter in lokalen Limit ist. Dieses Ergebnis impliziert auch, dass eine typische Skala für den lawinenenartig Transport inhärent für die ITG getriebene Turbulenz ist.

Declaration

The author declares that the materials presented in this thesis are his own work, unless explicitly stated otherwise. This thesis is based on

> Lippert, M., Rath, F. & Peeters, A. G. 2023 Size convergence of the E×B staircase pattern in flux tube simulations of ion temperature gradient-driven turbulence. *Phys. of Plasmas* **30** (7)

and is a further iteration of this publication (brief communication). It provides additional plots and paragraphs that were included in the publication. The brief communication can be found in Appendix **??**.

Additionally, the author states that every information, except data, regarding this thesis can be found under the GitHub Repository with the link `https://github.com/ManeLippert/Bachelorthesis-Shearingrate-Convergence`.

Contents

CHAPTER

1

Motivation

Ion temperature gradient driven turbulence close to marginal stability exhibits zonal flow pattern formation on mesoscales, so-called $\mathrm{E}\times\mathrm{B}$ staircase structures[3]. Such pattern formation has been observed in local gradient-driven flux-tube simulations[14,16], including collisions[21] and background $\mathrm{E}\times\mathrm{B}$ shear[16], local flux-driven realizations including mean electric field shear[17], as well as global gradient-driven[12,19,18] and global flux-driven[3,4,20,7,8] studies. In global studies, spanning a larger fraction of the minor radius, multiple radial repetitions of staircase structures are usually observed, with a typical pattern size of several ten Larmor radii. By contrast, in the aforementioned local studies the radial size of $\mathrm{E}\times\mathrm{B}$ staircase structures is always found to converge to the radial box size of the flux tube domain. The above observations lead to the question:

Does the basic pattern size always converges to the box size, or is there a typical mesoscale size inherent to staircase structures also in a local flux-tube description?

The latter case would imply that it is not necessarily global physics, i.e., profile effects, that set

(i) the radial size of the $\mathrm{E}\times\mathrm{B}$ staircase pattern

(ii) the scale of avalanche-like transport events.

These transport events are usually restricted to $\mathrm{E}\times\mathrm{B}$ staircase structures and considered as a nonlocal transport mechanism[3].

In this bachlor thesis the above question is addressed through a box size convergence scan of the same cases close to the nonlinear threshold for turbulence generation as studied in Ref. 14.

CHAPTER

Derivation Gyrokinetic Equations and Inductive Electric Field $E_{||}$

2

2.1 Charged Particle Motion in Magnetic and Electric Field

In magnetic confinement devices like the tokamak reactor, the charged particles experience forces caused by magnetic and electric fields which results in distinct motion under the associated force. Charged particles can be separated in species, e.g. electrons and ions, which will be later on not displayed in the governing equation. Throughout this thesis the charge q, the mass m or the temperature T indicate the quantities of a specific species, i.e., electrons or ions.

2.1.1 Particle Motion perpendicular to the magnetic field

Due to the Lorentz force, particles with a velocity component perpendicular to the homogenous magnetic field $v_\perp$ undergo a circular motion in the plane perpendicular to the magnetic field [Fig. 2.1(a)]. This type of motion has circular frequency, which is often referred to as *cyclotron frequency* and is defined as

$$\omega_\mathrm{c} = \frac{|q|B}{m} \ , \tag{2.1}$$

where m and q are the mass and the charge of the particle and B the strength of the magnetic field. The radius, the so called *Larmor radius*, of this motion is given by

$$\rho_\mathrm{L} = \frac{mv_\perp}{|q|B} \tag{2.2}$$

with the center often being referred to as *gyrocenter*. Note that since the Lorentz force depends on the species charge of the particle, the circulation direction is the opposite between electron in ions.

Due to Coulomb collisions the plasma gets thermalized. Together with the Maxwell-Boltzmann distribution the typical thermal velocity is

$$v_\mathrm{th} = \sqrt{\frac{2T}{m}} \ , \tag{2.3}$$

where T represents the species temperature. Based on the thermal velocity v_th the *thermal Larmor radius* gets introduced as

$$\rho_\mathrm{th} = \frac{mv_\mathrm{th}}{|q|B} \ .^{22} \tag{2.4}$$

2.1.2 Particle Motion parallel to the magnetic field

In absence of forces in the direction parallel to the magnetic field the particles can move freely in parallel direction to the homogenous magnetic field. The velocity of this motion is of order of the thermal velocity v_{th} and is dominated by electrons due to their lighter mass compared to ions ($v_{\mathrm{th,e}}/v_{\mathrm{th,i}} = 60$).

When an electric field with a component parallel to the magnetic field $E_\parallel$ influences the plasma the charged particles are accelerated by the electric force

$$F_{\parallel,E} = qE_\parallel \ . \tag{2.5}$$

The parallel motion follows then from the equation of motion. Here the direction of the motion also depends on the species type [Fig. 2.1(b)].

Since magnetic fields are not always homogenous, an inhomogeneous magnetic field with its gradient ∇B containing a component parallel to the magnetic field which is given by

$$\nabla_\parallel B = \frac{\mathbf{B}}{B} \cdot \nabla B \tag{2.6}$$

causes the force

$$F_{\parallel,\nabla_\parallel B} = -\frac{mv_\perp^2}{2B}\nabla_\parallel B = -\mu\nabla_\parallel B \ ; \qquad \mu = \frac{mv_\perp^2}{2B} \tag{2.7}$$

with *magnetic moment* μ. The magnetic moment μ is an adabatic invariant (constant of motion) if the variation of the magnetic field over time is smaller than the inverse of the cyclotron frequency ω_{c}^{-1} and the spatial variation is larger the Larmor radius ρ_{L}. The resulting force has its application in the mirror effect where a charged particle gets reflected due to this force [Fig. 2.1(c)].[22]

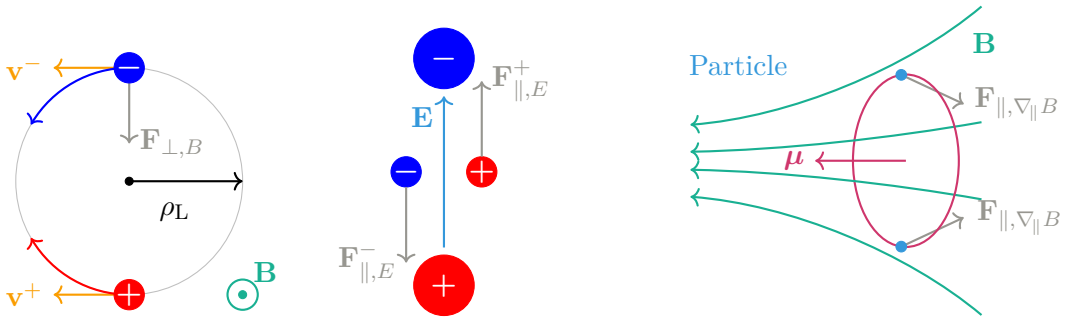

(a) **(b)** **(c)**

Figure 2.1: Forces acting on a charged particle:
- **(a)** Lorentz force $\mathbf{F}_{\perp,B}$ perpendicular to velocity $\mathbf{v}^\pm$ and magnetic field $\mathbf{B}$ which causes, circular motion with different directions for electron and ions, Lamor radius ρ_L and cyclotron frequency ω_c,
- **(b)** Electric force $\mathbf{F}^\pm_{\parallel,E}$ with electric field $\mathbf{E}$,
- **(c)** Mirror effect with force $\mathbf{F}_{\parallel,\nabla_\parallel B}$ and magnetic moment μ caused by an inhomogeneous magnetic field $\mathbf{B}$.

2.1.3 Drifts in the Gyrocenter

In the presence of a magnetic field (homogenous, inhomogeneous or perturbed) and electric fields the gyrocenter undergoes slow (compared to the thermal velocity v_{th}) drift motions perpendicular to the magnetic field. There are several examples for this drift motion. According to this thesis topic only the main three drift types will be covered in the following.

1. **E × B Drift:**
   If an electric field **E** with a perpendicular component together with the magnetic field **B** (both fields are homogenous) is present the acting Coulomb force and Lorentz force results into a drift of the gyrocenter with

   $$\mathbf{v}_E = \frac{\mathbf{E} \times \mathbf{B}}{B^2} \tag{2.8}$$

   which is called the E × B drift. Since both acting forces direction depends on the species type the direction of the E × B drift is for every species the same [Fig. 2.2(a)].
2. **∇B Drift:**
   Inhomogeneous magnetic field causes a gradient ∇B of the magnetic field. Because of that gradient the gyrocenter undergoes a ∇B drift defined by

   $$\mathbf{v}_{\nabla B} = \frac{m v_\perp^2}{2q} \frac{\mathbf{B} \times \nabla B}{B^3} \ . \tag{2.9}$$

   The gradient of the magnetic field ∇B varies thereby on scales larger compared to the Larmor radius. The direction of the ∇B drift depends on the species type [Fig. 2.2(b)].
3. **Curvature Drift:**
   Due to centrifugal force acting on the particle in a curved magnetic field the gyrocenter experiences a curvature drift according to

   $$\mathbf{v}_\kappa = \frac{m v_\parallel^2}{q} \frac{\mathbf{B} \times \boldsymbol{\kappa}}{B^2} = \frac{m v_\parallel^2}{q} \frac{\mathbf{B} \times \nabla B}{B^3} \ ; \qquad \boldsymbol{\kappa} = -(\mathbf{b} \cdot \nabla)\mathbf{b} = \frac{\nabla B}{B} \ , \tag{2.10}$$

   where **b** is the unit vector along the magnetic field. To obtain the result for the curvature $\boldsymbol{\kappa}$ in Eq. (2.10) the plasma pressure has to be small compared to the magnetic field strength B. In the form of Eq. (2.10) ∇B and curvature drift can be treated similarly.[22]

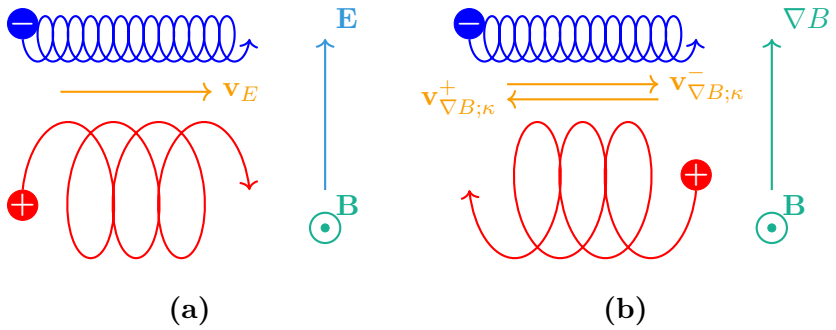

Figure 2.2: Dirft motion in gyrocenter:

(a) E × B Drift with drift velocity $\mathbf{v}_E$, electric field **E** and magnetic field **B**,

(b) ∇B Drift/Curvature Drift with drift velocity $\mathbf{v}^{\pm}_{\nabla B;\kappa}$, magnetic field **B** and gradient of the magnetic field ∇B.

2.2 Gyrokinetic Ordering

In the derivation of the gyrokinetic theory the aim is to decouple the effect of small-scale, small amplitude fluctuations of the plasma in the Langrangian. For this it is chosen to take the properties of fluctuations as small parameter, which will get in the ordering assumptions applied in gyrokinetic theory

$$\begin{aligned} \frac{|\mathbf{A_1}|}{|\mathbf{A_0}|} &\sim \frac{\Phi_1}{\Phi_0} \sim \epsilon_\delta \ll 1 \\ \rho\frac{\nabla B_0}{B_0} &\sim \rho\frac{\nabla E_0}{E_0} \sim \frac{\rho}{L_B} \sim \epsilon_B \ll 1 \\ k_\perp \rho &\sim \epsilon_\perp \sim 1 \\ \frac{\omega}{\omega_{\mathrm{L}}} &\sim \epsilon_\omega \ll 1 \end{aligned} \tag{2.11}$$

where $\mathbf{A}$ and Φ are the vector and scalar potentials, $\mathbf{B}$ and $\mathbf{E}$ are the magnetic and electric fields, ω and $k_\perp$ are the typical mode frequency and perpendicular wavenumber, ρ and ω_{L} are the Larmor radius and Larmor frequency and L_B the equilibrium magnetic length scale. The equilibrium quantities are denoted with 0 and the fluctuations with 1 subscript.

The above-mentioned equations state that fluctuations have a much smaller magnitude than the corresponding equilibrium values, their typical timescale is much slower than the Larmor frequency, their characteristic length scale is of the order of the Larmor radius, and it is typically much shorter the equilibrium spatial variation scale. Teh gyrokinetic equations are valid under these ordering assumptions.

The small parameters ϵ_δ, ϵ_B, $\epsilon_\perp$ and ϵ_ω are due to different physical but in practice it is assumed that they are of simular order and substitute them with one parameter. For the derivation of the gyrokinetic equations of GKW all derived equations are evaluated up to the first order of the ratio of the reference thermal Larmor radius ρ_{ref} and the equilibrium magnetic length scale L_B as small parameter and is defined as

$$\rho_\star = \frac{\rho_{\mathrm{ref}}}{L_B} = \frac{m_{\mathrm{ref}} v_{\mathrm{th,ref}}}{eB_{\mathrm{ref}}} \sim \epsilon_B \sim \epsilon_\delta \sim \epsilon_\omega \ . \tag{2.12}$$

2.3 Gyrokinetic Equations

2.3.1 Vlasov Equation

Because of the large number of particles in the fusion plasma a prediction on the basis of Newton-Maxwell dynamics results in an impossible task for simulation, but this problem can be solved with a statistical approach. For that the particle density distribution function $f(\mathbf{x}, \mathbf{v}, t)$ in the six dimensional phase space $\{\mathbf{x}, \mathbf{v}\}$ with the particles position $\mathbf{x}$ and velocity $\mathbf{v}$ is needed. Because collisions are happening at much smaller frequencies than the characteristic frequencies connected to turbulence, the collisionless model is often preferred[5] which results through evolution of the particle density distribution function in the *Vlasov equation*

$$\frac{\partial f}{\partial t} + \frac{\partial f}{\partial \mathbf{x}} \cdot \frac{\mathrm{d}\mathbf{x}}{\mathrm{d}t} + \frac{\partial f}{\partial \mathbf{v}} \cdot \frac{\mathrm{d}\mathbf{v}}{\mathrm{d}t} = 0 \ . \tag{2.13}$$

To obtain a closed system the Maxwell equations with the particle density n and current density j can be described with the distribution function as follows

$$n = \int \mathrm{d}\mathbf{v}\, f(\mathbf{x}, \mathbf{v}, t) \qquad j = q \int \mathrm{d}\mathbf{v}\, v f(\mathbf{x}, \mathbf{v}, t) \ , \tag{2.14}$$

which are then substituted into the Maxwell equations

$$\begin{aligned} \nabla \cdot \mathbf{B} &= 0 & \nabla \times \mathbf{B} &= \mu_0 \left(\sum_{\text{species}} j + \epsilon_0 \frac{\partial \mathbf{E}}{\partial t} \right) \\ \nabla \cdot \mathbf{E} &= \frac{1}{\epsilon_0} \sum_{\text{species}} qn & \nabla \times \mathbf{E} &= -\frac{\partial \mathbf{B}}{\partial t} \ . \end{aligned} \tag{2.15}$$

The Vlasov equation (2.13) in combination with the Maxwell equations (2.14) and (2.15) is the basis of the gyrokinetic model.[9]

2.3.2 Gyrokinetic Equation

For the description of charged particle behaviour in the tokamak device the *guidingcenter coordinates* are used [Fig. 2.3]. In this set of coordinates the guidingcenter follows the magnetic field with the parallel velocity $v_{\parallel}$. The gyro motion is described together with the magnetic moment $\mu = \frac{1}{2} m v_{\perp}/\omega_c$, the gyrocenter $\mathbf{X}$ and the gyro phase ζ which gives a parameter set of six quantities $\{\mathbf{X}, v_{\parallel}, \mu, \zeta\}$. The gyrocenter position $\mathbf{X}$ is expressed with the particle position $\mathbf{x}$ and the position Larmor radius vector $\boldsymbol{\rho}_{\mathbf{L}}$ as $\mathbf{X} = \mathbf{x} - \boldsymbol{\rho}_{\mathbf{L}}$.

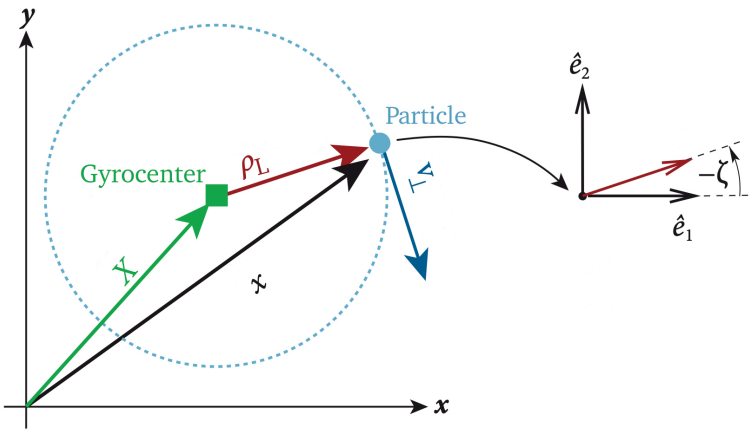

Figure 2.3: Sketch of guidingcenter coordinates where the charged particle performs a circular motion around the gyrocenter.[10]

In the next step the unperturbed Lagrangian is expressed through the guidingcenter coordinates. The particle velocity $\mathbf{v}$ is decomposed into a parallel component $v_{\parallel} = \mathbf{v} \cdot \mathbf{b}$ and a perpendicular component $v_{\perp} = |\mathbf{v} \times \mathbf{b}|$ which relates to the magnetic moment μ. As final step the Lagrangian is transformed into gyrocenter phase space, based on the so-called Lie perturbation theory. This method allows to eliminate the gyrophase-dependent contributions, rendering the gyrophase ζ an ignorable coordinate and the magnetic moment μ an exact constant of motion.[5,1,2] Taking everything into account the new coordinates of the Vlasov equation are $\{\mathbf{X}, v_{\parallel}, \mu\}$ which transforms the Vlasov equation into the *gyrokinetic equation*, describing the evolution of the gyrocenter distribution function.

$$\frac{\partial f}{\partial t} + \frac{\partial f}{\partial \mathbf{X}} \cdot \frac{\mathrm{d}\mathbf{X}}{\mathrm{d}t} + \frac{\partial f}{\partial v_{\parallel}} \cdot \frac{\mathrm{d}v_{\parallel}}{\mathrm{d}t} = 0 \ . \tag{2.16}$$

The time derivative of the magnetic moment μ is zero because the magnetic moment is an exact invariant.

2.3.3 δf Approximation and Local Limit

All simulations in this thesis are performed with GKW (Gyro Kinetic Workshop) which solves the gyrokinetic equation in the δf approximation and local limit. For the δf approximation the particle density distribution function f is seperated into perturbation δf and equilibrium f_0 (constant in time) as expressed in the gyrokinetic ordering (**??**). This is given by

$$f = f_0 + \delta f \qquad \delta f \sim \rho_* f_0 \ . \tag{2.17}$$

In GKW the equilibrium distribution function f_0 is set to the Maxwell distribution function. The perturbed distribution function δf is considered to vary perpendicular to the poloidal magnetic field of order of the Larmor radius while the equilibrium changes with the system size which results in the ordering

$$\nabla_\perp(\delta f) = \nabla_\perp(f_0) \ . \tag{2.18}$$

The δf approximation applies for global and local description where the latter is used in this thesis. The *local limit* on the other hand uses the spatial separation of equilibrium and perturbation and implies that all equilibrium and geometry quantities are considered constant over the radial extent of the simulation volume. Because of the tokamak symmetry all equilibrium quantities are also constant in the toroidal direction where the dependency of the equilibrium magnetic field on the poloidal angle is retrained in general.

In addition to this, in GKW the following coordinates get applied with the parameter $\mathbf{X} = \{x, y, s\}$. Here, x is the radial coordinate that labels the flux surfaces normalized by the thermal Larmor radius ρ_{th} and y labels the field lines and is an approximate binormal coordinate. Together with the coordinate s which parameterizes the length along the field lines and is referred to as the parallel coordinate these quantities form the Hamada coordinates[6]. This results in the coordinates $\{x, y, s, v_\parallel, \mu\}$. Combining the δf approximation and the Hamada coordinates the gyrokinetic equation can be formulated as follows

$$\frac{\partial g}{\partial t} + \mathbf{v}_\chi \cdot \nabla g + (v_\parallel \mathbf{b} + \mathbf{v}_{\text{D}}) \cdot \nabla(\delta f) - \frac{\mu B}{m} \frac{\mathbf{B} \cdot \nabla B}{B^2} \frac{\partial(\delta f)}{\partial v_\parallel} = S \ , \tag{2.19}$$

where g is a function which contains the perturbation δf and the equilibrium f_0. Furthermore, $\mathbf{v}_{\text{D}}$ and $\mathbf{v}_\chi$ are drift velocities which are caused by the inhomogeneous magnetic field ($\mathbf{v}_{\text{D}}$) and through the $\mathrm{E} \times \mathrm{B}$ drift ($\mathbf{v}_\chi$). The source term S contains the distribution function in the equilibrium f_0 and a correction term for the collisions as well as the energy injection term. Due to periodic boundary conditions in the radial direction the radial averaged gradients are fixed in time which is also referred to as *gradient-driven* approach.[13]

CHAPTER

3

Methods and Material

CHAPTER

4

Results and Discussion

The performed simulations for this chapter are documented in Appendix **??**.

CHAPTER

5

Conclusion

In this thesis the minimal resolution for simulations with GKW in the Cyclone Base parameter were observed in which the number of grid points for the parallel velocity $N_{\nu_\parallel}$ could be reduced from 64 to 48, which halfed the time until suppression of turbulence.

Additionally, the active development of a restart script in `python3` led to further convenience during the task of performing simulations on the `btrzx1` cluster.

Through careful tests this bachelor thesis confirms the radial size convergence of the $\mathrm{E} \times \mathrm{B}$ staircase pattern in local gyrokinetic flux tube simulations of ion temperature gradient (ITG)-driven turbulence. A mesoscale pattern size of $\sim 57 - 76\,\rho_{\mathrm{th}}$ is found to be intrinsic to ITG-driven turbulence for Cyclone Base Case parameters. This length scale is somewhat larger compared to results from global studies with finite ρ_*, which report of a few $10\,{\rho_{\mathrm{th}}}^3$, and has to be considered the proper mesoscale in the local limit $\rho_* \to 0$. The occurrence of this mesoscale implies that non-locality, in terms of Ref. 3, is inherent to ITG-driven turbulence, since avalanches are spatially organized by the $\mathrm{E} \times \mathrm{B}$ staircase pattern[12,3,15,14].

CHAPTER

6

Appendix

CHAPTER 7

Bibliography

[1] Cary, John R. 1981 Lie transform perturbation theory for Hamiltonian systems. *Physics Reports* **79** (2), 129–159.

[2] Cary, John R & Littlejohn, Robert G 1983 Noncanonical Hamiltonian mechanics and its application to magnetic field line flow. *Annals of Physics* **151** (1), 1–34.

[3] Dif-Pradalier, G., Diamond, P. H., Grandgirard, V., Sarazin, Y., Abiteboul, J., Garbet, X., Ghendrih, Ph., Strugarek, A., Ku, S. & Chang, C. S. 2010 On the validity of the local diffusive paradigm in turbulent plasma transport. *Phys. Rev. E* **82**, 025401.

[4] Dif-Pradalier, G., Hornung, G., Ghendrih, Ph., Sarazin, Y., Clairet, F., Vermare, L., Diamond, P. H., Abiteboul, J., Cartier-Michaud, T., Ehrlacher, C., Estève, D., Garbet, X., Grandgirard, V., Gürcan, Ö. D., Hennequin, P., Kosuga, Y., Latu, G., Maget, P., Morel, P., Norscini, C., Sabot, R. & Storelli, A. 2015 Finding the elusive E×B staircase in magnetized plasmas. *Phys. Rev. Lett.* **114**, 085004.

[5] Garbet, X., Idomura, Y., Villard, L. & Watanabe, T. H. 2010 Gyrokinetic simulations of turbulent transport. *Nuclear Fusion* **50** (4).

[6] Hamada, S. 1958 *Kakuyugo Kenkyu* **1**, 542.

[7] Kim, Y. J., Imadera, K., Kishimoto, Y. & Hahm, T. S. 2022 Transport events and E×B staircase in flux-driven gyrokinetic simulation of ion temperature gradient turbulence. *Journal of the Korean Physical Society* **81**, 636.

[8] Kishimoto, Y., Imadera, K., Ishizawa, A., Wang, W. & Li, J. Q. 2023 Characteristics of constrained turbulent transport in flux-driven toroidal plasmas. *Philosophical Transactions of the Royal Society A: Mathematical, Physical and Engineering Sciences* **381** (2242), 20210231.

[9] Krommes, John A. 2012 The Gyrokinetic Description of Microturbulence in Magnetized Plasmas. *Annual Review of Fluid Mechanics* .

[10] Krommes, John A. & Kim, Chang-Bae 2000 Interactions of disparate scales in drift-wave turbulence. *Phys. Rev. E* **62**, 8508–8539.

[11] Lippert, M., Rath, F. & Peeters, A. G. 2023 Size convergence of the E×B staircase pattern in flux tube simulations of ion temperature gradient-driven turbulence. *Phys. of Plasmas* **30** (7).

[12] McMillan, B. F., Jolliet, S., Tran, T. M., Villard, L., Bottino, A. & Angelino, P. 2009 Avalanchelike bursts in global gyrokinetic simulations. *Phys. of Plasmas* **16** (2), 022310.

[13] Peeters, A. G., Camenen, Y., Casson, F. J., Hornsby, W. A., Snodin, A. P., Strintzi, D. & Szepesi, G. 2009 The nonlinear gyro-kinetic flux tube code gkw. *Comput. Phys. Commun.* **180**, 2650.

[14] Peeters, A. G., Rath, F., Buchholz, R., Camenen, Y., Candy, J., Casson, F. J., Grosshauser, S. R., Hornsby, W. A., Strintzi, D. & Weikl, A. 2016 Gradient-driven flux-tube simulations of ion temperature gradient turbulence close to the non-linear threshold. *Phys. of Plasmas* **23** (8), 082517.

[15] Rath, F., Peeters, A. G., Buchholz, R., Grosshauser, S. R., Migliano, P., Weikl, A. & Strintzi, D. 2016 Comparison of gradient and flux driven gyro-kinetic turbulent transport. *Phys. of Plasmas* **23** (5), 052309.

[16] Rath, F., Peeters, A. G. & Weikl, A. 2021 Analysis of zonal flow pattern formation and the modification of staircase states by electron dynamics in gyrokinetic near marginal turbulence. *Phys. of Plasmas* **28** (7), 072305.

[17] Seiferling, F., Peeters, A. G., Grosshauser, S. R., Rath, F. & Weikl, A. 2019 The interplay of an external torque and e×b structure formation in tokamak plasmas. *Phys. of Plasmas* **26** (10), 102306.

[18] Seo, Janghoon, Jhang, Hogun & Kwon, Jae-Min 2022 Effects of light impurities on zonal flow activities and turbulent thermal transport. *Phys. of Plasmas* **29** (5), 052502.

[19] Villard, L, Angelino, P, Bottino, A, Brunner, S, Jolliet, S, McMillan, B F, Tran, T M & Vernay, T 2013 Global gyrokinetic ion temperature gradient turbulence simulations of iter. *Plasma Physics and Controlled Fusion* **55** (7), 074017.

[20] Wang, W., Kishimoto, Y., Imadera, K., Liu, H.R., Li, J.Q., Yagi, M. & Wang, Z.X. 2020 Statistical study for itg turbulent transport in flux-driven tokamak plasmas based on global gyro-kinetic simulation. *Nuclear Fusion* **60** (6), 066010.

[21] Weikl, A., Peeters, A. G., Rath, F., Grosshauser, S. R., Buchholz, R., Hornsby, W. A., Seiferling, F. & Strintzi, D. 2017 Ion temperature gradient turbulence close to the finite heat flux threshold. *Phys. of Plasmas* **24** (10), 102317.

[22] Wesson, John 2011 *Tokamaks*. Oxford: Oxford University Press.

Eidesstattliche Erklärung

Hiermit erkläre ich, Manuel Lippert, dass ich die vorliegende Arbeit selbständig und ohne Benutzung anderer als der angegebenen Hilfsmittel angefertigt habe. Alle Stellen,

die wörtlich oder sinngemäß aus veröffentlichten oder nicht veröffentlichten Schriften entnommen wurden, sind als solche kenntlich gemacht. Die Arbeit hat in gleicher oder

ähnlicher Form noch keiner anderen Prüfungsbehörde vorgelegen.

Bayreuth, den 30.06.2023

Manuel Lippert